Forest Ecology and Management 357 (2015) 239–247

Contents lists available at ScienceDirect

Forest Ecology and Management

journal homepage: www.elsevier.com/locate/foreco

Remote sensing proxies of productivity and moisture predict forest stand type and recovery rate following experimental harvest

Wiebe Nijland [a], Nicholas C. Coops [a,*], S. Ellen Macdonald [b], Scott E. Nielsen [b], Christopher W. Bater [c], Barry White [c], Jae Ogilvie [d], John Stadt [c]

[a] Department of Forest Resources Management, University of British Columbia, 2424 Main Mall, Vancouver, BC V6T 1Z4, Canada
[b] Department of Renewable Resources, University of Alberta, Edmonton T6G 2H1, Canada
[c] Forest Management Branch, Forestry Division, Alberta Agriculture and Forestry, 9920-108 Street, Edmonton, AB T5K 2M4, Canada
[d] Faculty of Forestry and Environmental Management, University of New Brunswick, 28 Dineen Drive Fredericton, New Brunswick E3B 6C3, Canada

ARTICLE INFO

Article history:
Received 17 June 2015
Received in revised form 19 August 2015
Accepted 19 August 2015

Keywords:
ALS
Lidar
Depth to water
EMEND
Landsat
Edatopic grid

ABSTRACT

Site productivity, as affected by soil nutrients and available moisture is often characterized using an edatopic grid. A challenge for forest ecologists and managers working across large areas and in complex landscapes is the need to identify spatially different ecological environments that follow an edatopic classification. Recent advances in remote sensing offer some potential approaches for mapping ecological environments and landscape conditions. It is now feasible to compile long temporal image sequences using Landsat imagery for reconstruction of forest stands and derivation of long term indices of landscape productivity; and the increasing proliferation of airborne laser scanning (ALS) technology also allows for the acquisition of detailed information on topographic elevation and vegetation structure with sub-meter accuracy. In a large area of boreal mixedwood forest in northwestern Alberta, Canada, we examined the utility of using Landsat-derived vegetation greenness (indicating productivity), and ALS-derived cartographic depth-to-water (indicating moisture), to determine forest cover type and vegetation responses following variable retention harvesting. Our results demonstrate that both long-term image sequences from Landsat and ALS-derived topography and vegetation structure act as proxies for edatopic grid components, and are well-suited to differentiating forest cover types. Deciduous-dominated, deciduous-dominated with conifer understory, mixed, and conifer-dominated forests were generally distributed (in order) across a gradient of increasing moisture and decreasing greenness. Landscape greenness was the strongest predictor of vegetation regrowth after disturbance, followed by depth to water and other terrain factors, such as elevation and slope. New advances in, and complementary use of, different remotely sensed information provides a better understanding of both the landscape-scale distribution of forest cover types and patterns of vegetation regrowth following disturbance.

© 2015 Elsevier B.V. All rights reserved.

1. Introduction

It has long been recognized that interrelationships between soils and climate are key environmental factors controlling plant establishment, survival and growth (Major, 1951). This understanding has led to the development of ecosystem-based classification systems, which are designed to help organize our understanding of forest distribution and productivity (Beckingham and Archibald, 1996). Climate is recognized as the most fundamental environmental factor influencing species distribution and productivity in terrestrial ecosystems (Pojar et al., 1987) and it therefore is often viewed as having an overarching role in any classification system. Soil nutrient regime provides an indication of the availability of soil nutrients to plants (Hylander and Dynesius, 2006; Major, 1951) and is a function of a number of different soil properties (Landsberg, 1996). Soil moisture regime controls the amount of soil water available for transpiration by plants and evaporation throughout the year; this varies as a function of topography and soil type, ranging across a landscape from very dry to constantly wet (Murphy et al., 2009, 2008a; Pojar et al., 1987; Seibert et al., 2007).

The edatopic grid concept (Pogrebnjak, 1929; Rysin, 1982) is a useful tool for describing relationships between the occurrence of particular plant species, and the soil moisture and nutrient status

* Corresponding author.
E-mail addresses: irss.ubc@wiebenijland.nl (W. Nijland), nicholas.coops@ubc.ca (N.C. Coops), ellen.macdonald@ualberta.ca (S.E. Macdonald), scott.nielsen@ualberta.ca (S.E. Nielsen), chris.bater@gov.ab.ca (C.W. Bater), barry.white@gov.ab.ca (B. White), jae.ogilvie@unb.ca (J. Ogilvie), john.stadt@gov.ab.ca (J. Stadt).

http://dx.doi.org/10.1016/j.foreco.2015.08.027
0378-1127/© 2015 Elsevier B.V. All rights reserved.

of a site within a given climatic context. The grid represents an abstract landscape that includes all combinations of moisture and nutrient availability within a region of homogenous climate. The landscape represented are not real, rather conceptual, to help ecologists translate species associations that would occur across a physical landscape such as a river valley (Haeussler, 2011). Edatopic grids are commonly used in Canada as the basis for ecosystem classification and is the basis for a number of Provincial systems including the Biogeoclimatic Ecosystem Classification (BEC) system in British Columbia (Pojar et al., 1987) and the ecosite classification system in Alberta (Beckingham and Archibald, 1996). Mapping ecological classes across the edatopic grid represents a key challenge in mapping landscapes, especially across large areas and in complex landscapes (Clark and Palmer, 1999). Field-based mapping is costly and time consuming, typically providing only a small spatial sample of the landscape of interest. Scaling up plots across a suite of edaphic modifiers is critical, but in many cases data on these come in a variety of formats, scales, vintages, and levels of accuracy and detail (Ise and Sato, 2008). These challenges have limited the spatial mapping of ecological classes, which in turn has limited the utility of ecosystem classification systems to forest and land managers.

Remote sensing products often form the basis for extrapolation of ecosystem classification over the landscape (Coops et al., 2008). Aerial photography and trained interpreters are often used to delineate polygons of similar stand structure, species composition and land form, which in turn form the basis for the initial stratification. These maps are often produced at a fine spatial scale (<1:20,000) to ensure they are useful for forest managers working on operational issues. However, the significant manual interpretive effort and the cost of aerial photography have made these local mapping initiatives expensive. Remote sensing-derived forest cover layers are available at coarser spatial scales. For example, the Earth Observation for Sustainable Development of Forests (EOSD) defines deciduous, coniferous, and mixed forested types by multiple density categories (Wulder et al., 2008b). While improvements in optical remote sensing have led to increases in the predictive power of land cover classifications, analysis of single images at single snapshots in time cannot fully represent the complex dynamics of stand and canopy conditions, particularity in areas where forest management regularly changes the structure of the forest (Hermosilla et al., 2015). Although optical imagery is well-suited to detecting forest cover variation, the lack of three-dimensional information further limits its usefulness for assessing structural measures of forests (Lefsky et al., 1999).

The past decade has seen significant advances in the use of remote sensing technology on two fronts. First, due to American data policy changes in 2008, all new and archived Landsat images held by the United States Geological Survey (USGS) have become freely available (Wulder et al., 2012). As a result, users can now compile long temporal image sequences, and therefore are not restricted to analysis of single scenes due to costs limitations (Loveland and Dwyer, 2012). Further, advances in cloud screening (Zhu and Woodcock, 2012) and atmospheric correction (Masek et al., 2006) have led to a drastic increase in the volume of Landsat data used in disturbance detection studies, both in terms of spatial and temporal extent (Wulder et al., 2012). With the development of approaches to analyze time-series sequences of Landsat images (e.g., Huang et al., 2010; Kennedy et al., 2010; Zhu et al., 2012), it is now possible to reconstruct the recent history of forest disturbances and to assess long term productivity of a landscape.

A second key advance in remote sensing technology is the increasing use of airborne laser scanning (ALS) technology, which directly measures the three-dimensional distribution of vegetation. Airborne laser scanning is especially valuable for characterizing forest canopies, and may be used to capture structural attributes of individual trees (Lefsky et al., 1999). Airborne laser scanning systems typically acquire data at altitudes between 500 and 3000 m above ground level and, (Hilker et al., 2010) compared to ground-based survey methods, effectively cover large areas at relatively low cost (Coops et al., 2007; Naesset, 1997; Wulder et al., 2008a). Airborne laser scanning can directly measure the three-dimensional distribution of vegetation components as well as terrain morphology, providing information at high spatial resolution (e.g. sub-meter) related to topographic elevation, as well as vegetation height, cover, and other aspects of canopy structure. High spatial resolution digital elevation models (DEMs) derived from ALS also allow for fine-scale estimation of variables such as slope, aspect, terrain curvature, and other, more complex topographic indices related to water availability. For example, Murphy et al. (2008a) described the estimation of depth to water across the landscape using ALS-derived DEMs.

High resolution terrain information can be used to generate models related to soil moisture, while long term information on landscape greenness from optical data derived from Landsat imagery can be used as a surrogate for productivity. Together, parallel advances of these two contemporary remote sensing systems offer a unique opportunity to examine how these technologies can be used to spatially map different ecological classes across the edatopic grid.

The objective of this paper was to assess the utility of these emerging remote sensing technologies for describing variation in moisture and productivity regimes across the landscape, and to examine structural responses of vegetation to forest disturbance. We focused our analysis on the Ecosystem Management Emulating Natural Disturbance (EMEND) experimental site located in the mixedwood boreal forest of northern Alberta, Canada. The site includes a range of tree species associations as well as variable-retention harvesting treatments. Variations in stand types and retention levels have led to a range of different forest structures. We first explore the utility of Landsat-derived vegetation greenness as an indicator of productivity, and the use of ALS-derived depth to water as an indicator of moisture regime. We then examined two metrics of forest structure (canopy and understory cover) and their response to variable retention harvesting along moisture and productivity gradients. Finally, we discuss further development of these types of indicators for general ecosystem site mapping and forest ecosystem classification.

2. Methods

2.1. The EMEND site

The study was conducted at the EMEND (Ecosystem Management Emulating Natural Disturbance) experimental site in northwestern Alberta, Canada (56°46′13″N, 118°22′28″W). This 1080 ha experiment is within the Lower Boreal Highlands Subregion of the Boreal Forest Natural Region in Alberta (Natural Regions Committee, 2006). The subregion has a continental climate with mean warmest and coldest month temperatures of 15 °C and −20 °C, respectively, and mean annual precipitation of ~495 mm, two-thirds of which falls as rain (Natural Regions Committee, 2006). Soils in the area are predominantly fine-textured luvisols formed on glacio-lacustrine deposits (Kishchuk et al., 2014). Mixedwoods are common to the boreal forest of Canada (Bergeron et al., 2014). The dominant tree species are *Populus tremuloides* Michx (trembling aspen), *Populus balsamifera* L. (balsam poplar), and *Picea glauca* Moench (white spruce). In the absence of suppression activities, fire return cycle would be short, with large individual fire events (Bergeron et al., 2014); differences in fire size and frequency are key drivers of vegetation composi-

tion, structure, and dynamics (Kneeshaw and Gauthier, 2003). Fire events often leave structural legacies of both live and dead trees, reducing the contrast between disturbed and undisturbed stands (Hansen et al., 1991; Hunter, 1993). While fire has historically been the dominant disturbance in boreal mixedwoods (Bergeron et al., 2001), forest harvesting is now an important agent of disturbance in many parts of the landscape. Harvesting is increasingly based on a natural-disturbance-related paradigm of ecosystem management, which posits that disturbances emulating natural ecosystem processes will maintain high levels of biodiversity (Buddle et al., 2006; Levin, 2012), habitat connectivity (Saunders et al., 1991) and habitat heterogeneity (Turner, 1989).

The EMEND experiment was established in 1998 to assess a range of management practices designed to maintain ecosystem structure and function within the context of natural-disturbance-based ecosystem management (Volney et al., 1999). The overall design and motivations of the study are well described by others (Hannam et al., 2006, 2005; Jerabkova et al., 2006; Lazaruk et al., 2005; Lindo and Visser, 2003; Macdonald and Fenniak, 2007). The design of EMEND focuses on six variable retention harvesting treatments (clearcut or 2% retention, 10%, 20%, 50%, 75% dispersed green-tree retention harvesting, and an un-harvested control) applied to four major forest cover types characteristic of the mixedwood boreal (Volney et al., 1999): deciduous-dominated (DD) composed of 80–95% trembling aspen; deciduous-dominated with coniferous understory (DU) composed of 80–95% trembling aspen with white spruce understory at 60–80% of full stocking; mixed coniferous and deciduous (MX) composed of 35–65% of each; and coniferous-dominated (CD) composed of 80–95% white spruce (Work et al., 2004) (Fig. 1). The four forest cover-types, represent an undisturbed boreal mixedwood successional chronosequence as the first factor of the experimental design. Each harvest treatment was applied to three 10 ha compartments within each forest type. The stands selected for the study all had mature forest cover with stand replacing disturbances occurring in the last century (establishment dates 1842–1903 AD). Within each compartment, six permanent sample plots (10 m by 40 m) were established and have been regularly monitored for a wide variety of ecological attributes, including forest productivity, and biodiversity related to a variety of organisms.

2.2. Remote sensing datasets

2.2.1. ALS acquisition

Discrete ALS data were acquired in August 2008 (the tenth growing season following harvest) using a Leica ALS50-II sensor flying at a mean altitude of 2000 m above ground. Ground and non-ground returns were separated using Terrascan v 0.6 (Terrasolid, Helsinki, Finland) (Kraus and Pfeifer, 1998). A bare Earth DEM was generated from the ground returns by creating a triangulated irregular network, which was in turn rasterized at a spatial resolution of 1.0 m. The average density of the ALS data was 2 pts/m^2. Two sets of attributes were utilized from the ALS data: (1) terrain information and cartographic depth to water; and (2) height metrics related to vegetation structure.

2.2.2. Depth to water

White et al. (2012) describe the derivation of depth to water estimates using the Wet Area Mapping (WAM) algorithm detailed by Murphy et al. (2008b). The approach focuses on defining wet soils and areas close to lakes, streams, and mires as they are particularity susceptible to soil disturbances (e.g., rutting and compaction) (Ågren et al., 2014; Murphy et al., 2008a). The depth to water estimates were produced following the wet areas mapping approach described by White et al. (2012) and includes: (1) creating a continuous routing flow (Hornberger and Boyer, 1995; Jenson and Domingue, 1988) of water over the ALS-derived terrain model, using a combination of depression filling and breaching; (2), predicting the locations of streams on the surface based on a flow accumulation threshold; (3) interpolating the water table between surface features and calculating the cartographic depth to water. The methodology does not actually detect the depth to water table using the ALS data, rather from the very high spatial resolution DEM, patterns of water flow are derived allowing estimation of where the water table should be present across the examined landscape. The main adjustable parameter was the flow accumulation threshold which varied from 0.5 to 16 ha (White et al., 2012) with spatial layers available at six different catchment scales (0.5, 1.0, 4.0, 8.0. 12.0 and 16.0 ha). Optimal flow accumulation threshold depends on factors such as soil permeability and the specific application of the wet area map. For mechanical (e.g. road building) applications the value was determined to be 4 ha in our study area (White et al., 2012). However, since the maps are a static representation of an inherently dynamical process, this threshold may be suboptimal for forest productivity or ecological applications as presented in this study. To find the optimal threshold we compare the model AIC of the six different settings against forest productivity and structure. The evaluation is done based on individual plots and compartment averages to see the effects of upscaling and generalization on the optimal value.

2.2.3. Measures of vegetation structure

Metrics characterizing vegetation structure can be derived from non-ground returns in the ALS point cloud which are expressed in height above the ground surface. A set of plot-based height metrics were calculated using the area-based approach (White et al., 2013), including the height of percentiles of non-ground returns (10, 20, 30, 40, 50, 60, 70, 80, 90, and 95 percentiles), and canopy return density over a range of relative heights – specifically the proportion of laser returns in ten height intervals (D0, D1, D2, D3, D4, D5, D6, D7, D8, D9) between 0.5 m (D0) and the 95th (D9) percentile of maximum height (Næsset and Gobakken, 2008; Næsset, 2004). From these, we assumed the 95th percentile height represented maximum stand height, percent returns above 2 m to represent total canopy cover, and percent returns between 0.5 and 6 m to represent vegetation regrowth (Nijland et al., 2015). Previous research has shown that maximum stand height derived from ALS is relatively insensitive to variable harvest regimes and is therefore a good indicator of overall site productivity (Nijland et al., 2015). Understory, vegetation regrowth, and canopy cover will be highly sensitive to variable retention harvest treatment.

2.2.4. Landsat data and pre-processing

Landsat Thematic Mapper (TM) and Enhanced Thematic Mapper (ETM) images acquired during the growing seasons (June 1st–August 31st, Hermosilla et al., 2015) between 1990 and 2011 were downloaded from the USGS (Earth Explorer) (WRS 2 Tiles: p046r020, p047r020). Images were pre-processed to surface reflectance using the Landsat Ecosystem Disturbance Adaptive Processing System (LEDAPS) atmosphere correction tool (Masek et al., 2008; Vermote et al., 1997) and cloud, cloud shadow, snow and water were screened using the Fmask algorithm (Zhu and Woodcock, 2012). We derived a productivity indicator from the temporal sequence of images as the maximum normalized difference vegetation index (NDVI) (Tucker, 1979) from 1990 to 1998, capturing productivity of the forest before the harvest treatments. Previous studies have shown that taking the maximum greenness value of an image sequence minimizes atmospheric variation, such as cloud and other confounding conditions (e.g. snow, pasture, crops and exposed soil) (Coops et al., 1997). Furthermore, by extracting the maximum NDVI value across a decade, we are closer to detecting vegetation productivity at or near its peak, essentially

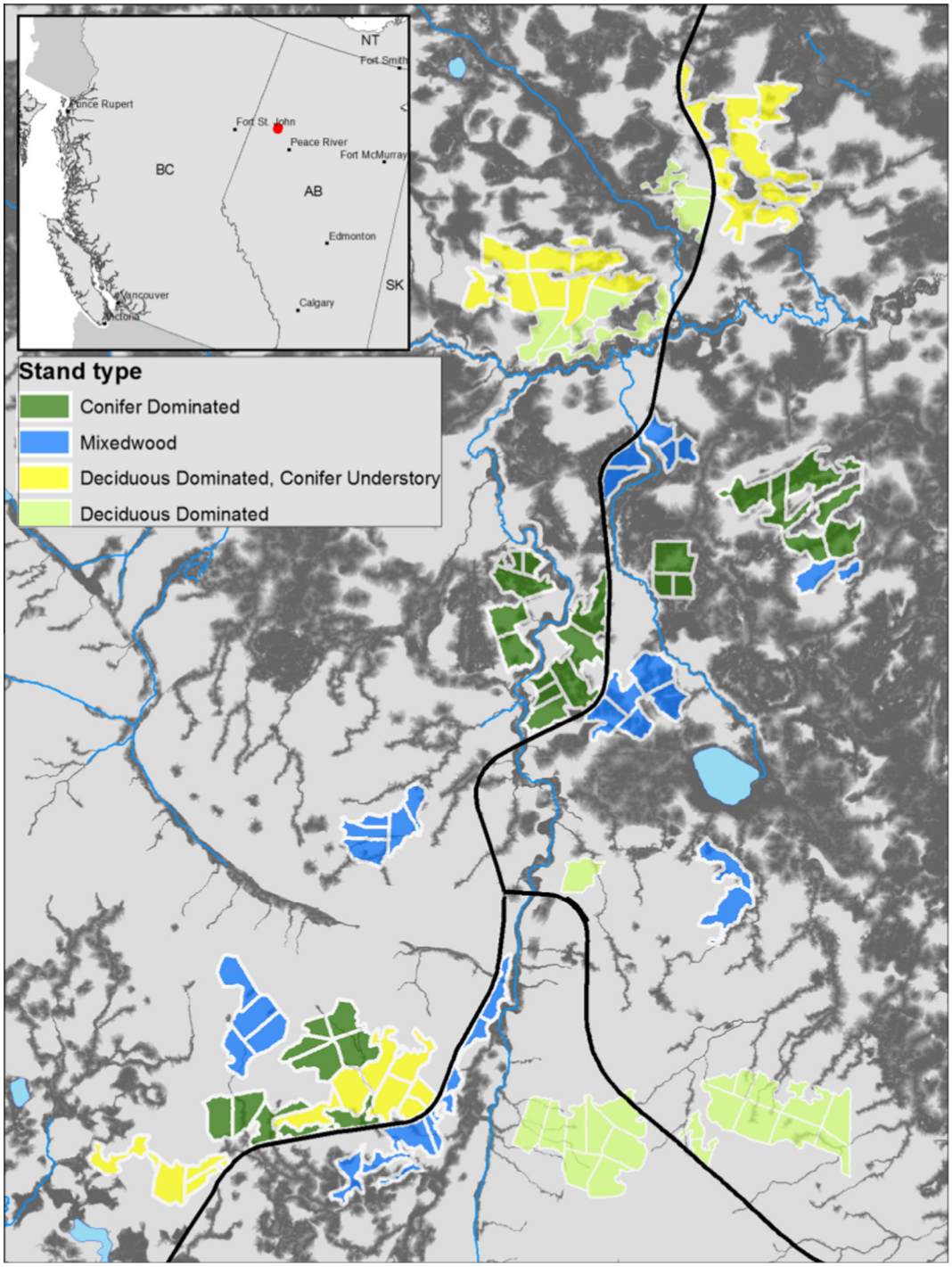

Fig. 1. Overview map of the EMEND study site. Depth to water from the wet areas mapping (based on airborne laser scanning data) is shown in the background with darker shades of gray signifying moist sites.

representing an index of the productive capability of the site (Coops et al., 1997; Goward et al., 1985).

2.3. Analysis approach

A summary of the different datasets utilized in the study is shown in Table 1. We extracted the remote sensing attributes at two spatial scales matching the EMEND experimental design, calculating metrics for both plots and compartments. For the plot scale, the remote sensing variables were averaged within the 40×10 m plot boundaries with six replicates per compartment (three compartments per forest type per harvesting treatment; ($n = 6$ plots $\times$ 72 compartments)). For the compartment scale analysis we averaged the remote sensing data across each compartment ($n = 72$ compartments).

To determine the flow accumulation catchment area to use for calculating depth to water, we compared generalized linear models for metrics of vegetation structure (based on ALS) and productivity (based on maximum NDVI) as a function of depth to water calculated using different catchment area thresholds; this was done at

Table 1
Base statistics (minimum, maximum, mean and standard deviation) for response and predictor variables used in this study, and the source of data (field collection, Landsat, or airborne laser scanning (ALS). Forest type and variable retention harvesting treatment were included as categorical variables in the models.

Type	Variable	Units	Min	Max	Mean	Standard deviation
Landsat	Maximum pre-harvest NDVI	–	0.76	0.89	0.85	0.03
ALS vegetation	Tree height (P95)	m	3.2	32.7	19.4	7.9
ALS vegetation	Canopy cover (above 2 m)	%	4.0	91.3	54.7	17.5
ALS vegetation	Understory regeneration (0.5–6 m)	%	4.1	91.1	50.4	26.8
ALS terrain	Elevation	m	689	868	748	48
AlS terrain	Slope[a]	deg	0.9	16.1	3.6	2.2
ALS terrain	Depth to water[a]	m	0.0	29.1	3.2	4.7
	Stand type (tree species composition) [b]			CD, MX, DU, DD		
	Treatment (harvest residual)	%		Clear cut, 10, 20, 50, 75, Control		

[a] *Note:* Depth to water and slope were log-transformed in all models.
[b] CD: conifer-dominated, MX: mixed conifer-deciduous; DU: deciduous dominated with conifer understory; DD: deciduous dominated.

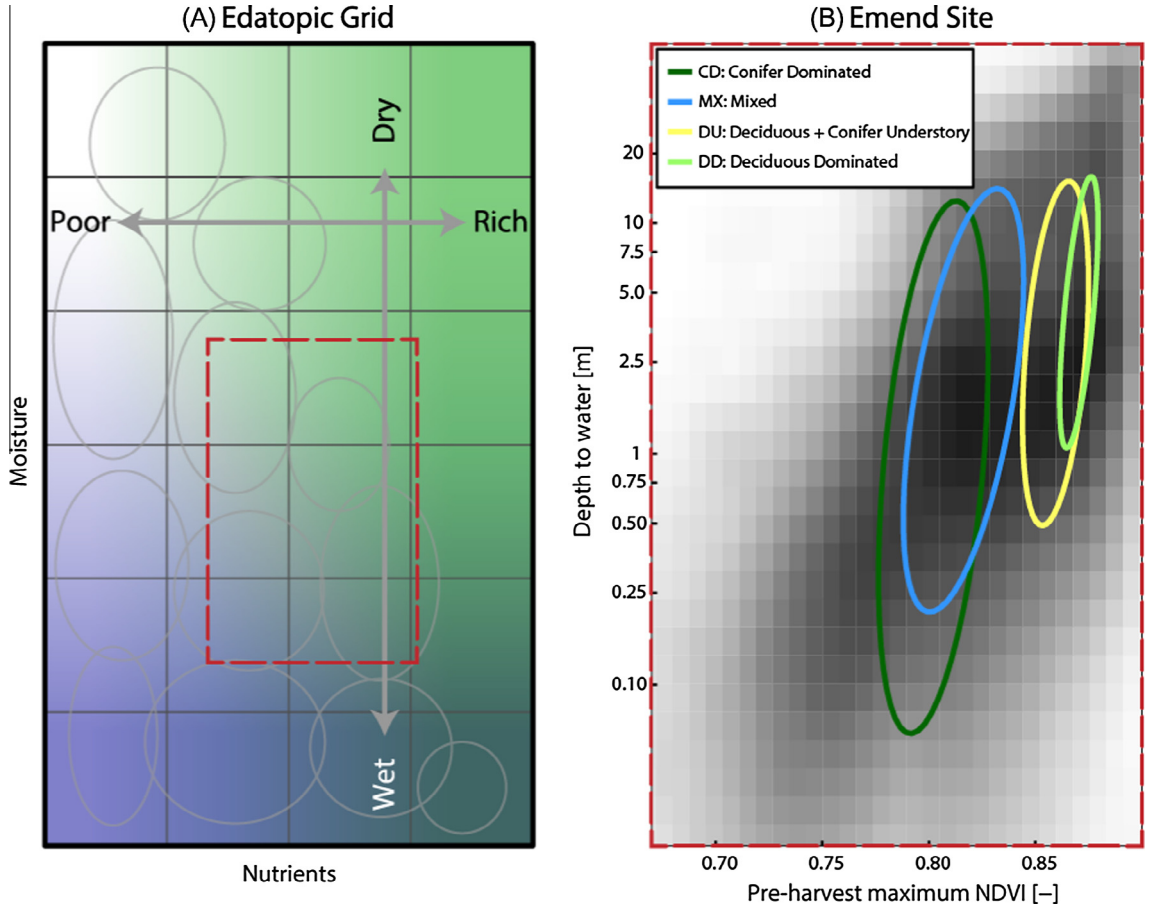

Fig. 2. (A) General structure of an Edatopic grid, the red box shows the area of the grid that the EMEND experimental site covers. (B) Ellipses showing the 95% confidence interval of the four different forest cover types within the study area across gradients of moisture (depth-to-water) and productivity (maximum NDVI). Shading indicated the prevalence of conditions in the entire (1080 ha) area as shown in Fig 1. (For interpretation of the references to color in this figure legend, the reader is referred to the web version of this article.)

both the plot and the compartment scales. In all models, stand type is included as a predictor variable to account for major differences between them. For models developed at the individual plot scale, compartment was included as a random factor, as plots within a compartment are not independent. To compare the models we used the Akaike Information Criterion (AIC) (Akaike, 1973) and compared the difference between each model to determine the most supported model (change in AIC or ΔAIC) for each dependent variable.

We determined the effect of a range of moisture estimates (as determined by the cartographic depth to water), site productivity (estimated from landscape greenness; maximum NDVI), and topography (slope and elevation) on vegetation structure (ALS total canopy cover >2 m) and vegetation regrowth (ALS proportion of returns between 0.5 and 6 m) by estimating mixed effects models with treatment and forest cover type as grouping variables. We constructed models for each of the four predictor variables individually, and then one model including depth to water plus the best predictor variable from among the others. Models were compared using ΔAIC, and the best model was selected based on the lowest AIC. Depth to water and slope were log transformed for these analyses to improve linearity. These analyses were conducted at the

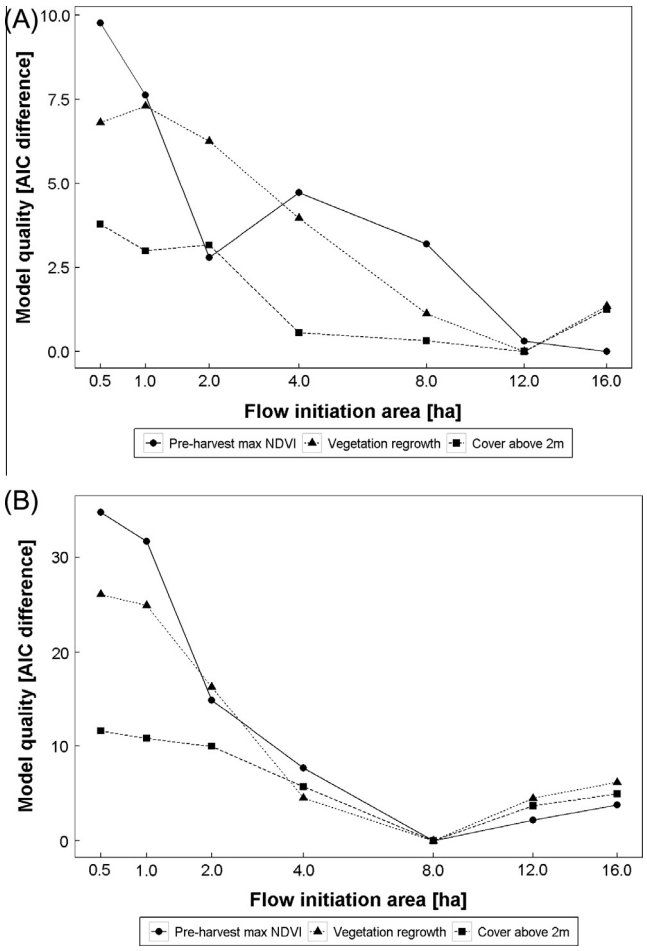

Fig. 3. Comparison of model strength, assessed as change in AIC, among flow initiation catchment sizes used to calculate depth to water. Given are ΔAIC values for four response variables: pre- and post-harvest NDVI, total canopy cover (>2 m height) and vegetation regrowth (0.5–6 m height). (A): Compartment averages; and (B): Individual plots.

individual plot scale, and thus compartment was included as a random factor to account for a lack of independence among plots within each compartment.

3. Results

Fig. 2a shows the conventional edatopic grid with the general position of the EMEND site indicated with the red dashed box. Fig. 2b expands this area and expresses productivity as the Landsat derived maximum pre-harvest NDVI, and moisture as ALS derived depth to water. The four forest cover types were distributed across gradients of moisture and productivity. Both the deciduous dominated stands and deciduous-dominated with conifer understory were constrained towards the drier end of the moisture gradient, while the conifer and the mixed stands covered a very large gradient of moisture, being more prevalent in moderately wet sites (Fig. 2b). The broader landscape contained some areas which were drier than the EMEND plots (with the same level of overall greenness), but a larger proportion of sites were wetter with low productivity, as the experimental compartments and plots were established in merchantable stands. Thus, the sampled forest stands represent relatively productive sub-mesic to sub-hygrid site types within the boreal mixedwood forest landscape. Sites with very high moisture (i.e., peatlands dominated by black spruce (*Picae mariana* (Mill.) BSP) and tamarack Larix laricina (Du Roi) K. Koch), or open bogs fell outside the sample domain.

To find the optimal flow initiation area we compared the predictive capacity of depth to water with different thresholds for vegetation structure and productivity. At both the compartment and plot scale, as the flow initiation area increased, the strength of the relationship between vegetation structure or productivity and depth to water increased, expressed as a lower AIC (Fig. 3). At the compartment scale there was no clear optimum catchment area, with some vegetation attributes best corresponding to 12 ha and some to 16 ha scales (Fig 3a). For the analysis at the individual plot scale, vegetation attributes were best matched with the depth to water computed with an 8 ha flow accumulation area (Fig 3b). Based on this analysis we used depth to water from the 8 ha flow initiation area and the individual plot scale in subsequent analyses.

Site productivity (pre-harvest maximum NDVI) was negatively related to moisture (i.e. positively correlated with depth to water) for all forest types (Fig. 4). Deciduous dominated stands had the highest productivity, followed by the deciduous-dominated with conifer understory, then mixed and finally conifer-dominated stands (Figs. 2b and 4). Correlation between productivity and moisture was strongest for the conifer and mixed stands compared to the two deciduous-dominated forest types (Fig. 4). Further, plots in the mixed and conifer-dominated forest types covered a larger gradient of both moisture and productivity than did the deciduous dominated stands.

For models of both total canopy cover and vegetation re-growth (both as estimated from ALS), pre-treatment maximum NDVI was the strongest single predictor, indicating satellite-derived indices of productivity better predict vegetation response to disturbance (i.e. variable-retention harvesting treatments) than do terrain metrics such as depth to water (Table 2). The next strongest variable was depth to water, which had a greater effect in both of the models compared to other ALS derived terrain metrics such as elevation or slope. As a result, for both response variables, the best model included as predictors both the pre-treatment NDVI and depth to water (Table 2) with an RMSE of 24.7% and 10.9% for understory regrowth and canopy cover respectively.

Both total canopy cover and vegetation regrowth were positively related to moisture (depth to water) and productivity (maximum pre-treatment NDVI) (Table 2; Fig. 5). As above, there was a consistent trend for the deciduous-dominated and deciduous with coniferous understory stands to occur on drier sites and to exhibit higher NDVI values compared to the coniferous and mixed stands.

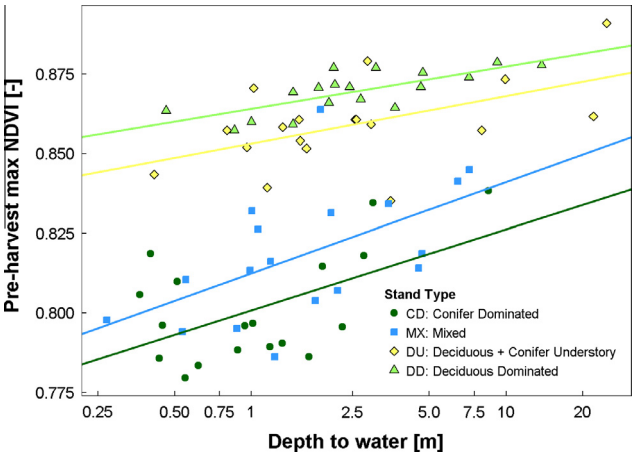

Fig. 4. Productivity (pre-harvest NDVI) as a function of depth to water (derived from airborne laser scanning) for the four forest cover types based on the individual plot analysis.

Table 2
Comparison of the different light detection and ranging (ALS) – based models of understory regeneration and canopy cover as predicted by variable retention harvesting treatment, forest stand type, and predictor variables derived from Landsat (pre-harvest NDVI) or ALS (elevation, slope, depth to water). Models were compared using Akaike's Information Criterion (AIC) and difference in AIC (ΔAIC); also given is the Akaike Weight (W_i). The best model for each response variable is in bold.

Model	AIC	ΔAIC	W_i
Understory ~ Treatment + StandType	217	53.5	<0.0001
Understory ~ Treatment + StandType + DTW[a]	183	20.2	<0.0001
Understory ~ Treatment + StandType + Elevation	188	24.7	<0.0001
Understory ~ Treatment + StandType + Slope[a]	205	42.4	<0.0001
Understory ~ Treatment + StandType + MaxNDVI	179	16.2	0.00
Understory ~ Treatment + StandType + MaxNDVI + DTW[a]	**163**	**0**	**0.99**
CanCover[b] ~ Treatment + StandType	3460	65.9	<0.0001
CanCover ~ Treatment + StandType + DTW[a]	3425	30.8	<0.0001
CanCover ~ Treatment + StandType + Elevation	3456	62.0	<0.0001
CanCover ~ Treatment + StandType + Slope[a]	3459	65.3	<0.0001
CanCover ~ Treatment + StandType + MaxNDVI	3407	12.6	0.00
CanCover ~ Treatment + StandType + MaxNDVI + DTW[a]	**3394**	**0**	**0.99**

[a] Depth to water and slope were log-transformed for all models.
[b] Canopy cover was positively related to Max NDVI and depth to water.

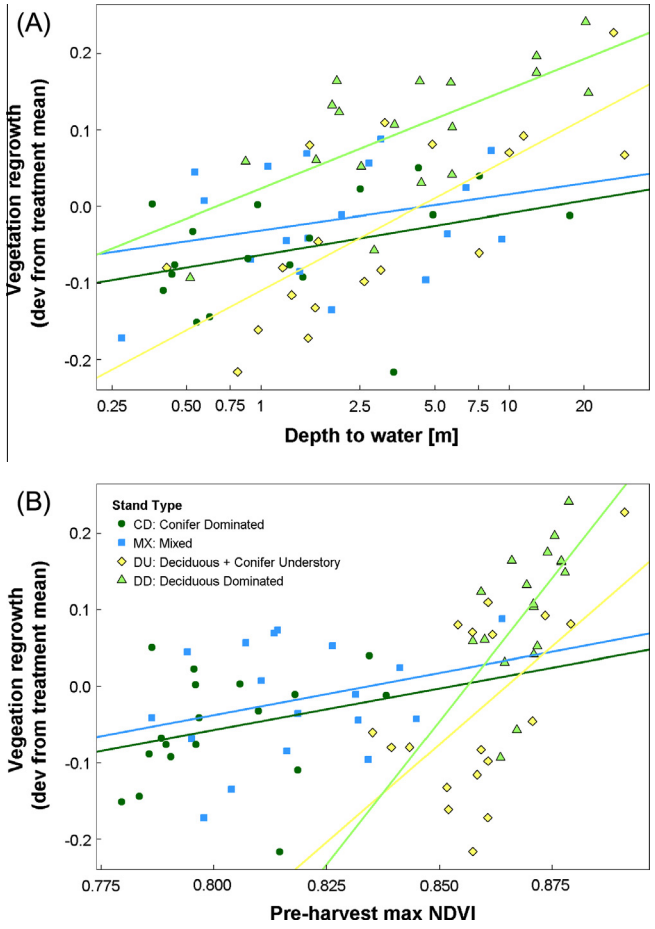

Fig. 5. Influence of (A) site moisture (depth to water; note the log scale), and (B) pre-harvest productivity (NDVI) on post-harvest regrowth (0.5–6 m height as determined by airborne laser scanning; shown as deviation from treatment mean) for each of the four forest types.

Vegetation regrowth was greater for the two deciduous-dominated stand types and also for stands that were drier (Fig. 5a). Wetter sites, in all cases, had below average vegetation regrowth, irrespective of forest type. The positive relationship between vegetation regrowth and site productivity (pre-treatment NDVI) was much stronger for the two deciduous-dominated forest types as compared to mixed and conifer-dominated stands (Fig. 5b).

4. Discussion

In this paper we examined the efficacy of using remote sensing proxies of productivity and moisture to model and understand responses of mixedwood forests to partial harvest treatments. We used maximum NDVI extracted from a Landsat time series as an indicator of forest productivity, while ALS-derived depth to water provided a useful indicator of moisture regime. For the second objective we examined two metrics related to forest structure (canopy cover and understory regrowth) and their response to variable retention harvesting along moisture and productivity gradients. We found that NDVI and depth to water, alone or combined, correlated strongly with fine scale forest dynamics following disturbance with greater recovery on productive sites and drier areas.

Usefulness of the depth to water, as derived from the wet-areas mapping algorithm, is affected by the spatial resolution, accuracy, and other limitations of the available DEM. The high spatial resolution DEMs derived from ALS data are ideally suited to delineate lower-order streams, but these DEMs are still limited to modeling surface or near-surface flow pathways (i.e. water pathways affected by topography). We reiterate that the ALS data is not directly detecting water within the soil of the landscape rather models patterns of water flow from high spatial resolution DEM. As a result, the interpolation method between stream channels detected from the DEM by the ALS may not accurately represent the water table, especially in areas further away from surface water and in steep topography, and must not be interpreted as the actual water table in those areas. However, higher values of depth to water only occur on steeper slopes which are generally better drained than flat areas; it is therefore not surprising that the relation between forest processes and depth to water is strong in those areas as highlighted in this study. In addition, very dense ground vegetation and thick sphagnum moss can limit ALS ground return numbers and accuracy, and mask some of the fine scale topographic variation represented in the DEMs'.

Another factor is the varying flow accumulation area thresholds for initiating digital stream networks and detecting wet areas. Ågren et al. (2014) found that different optimum area thresholds within the Krycklan watershed affected predictions. For example, low infiltration areas in fine glacial till-derived landforms were best predicted with a 1–2 ha flow accumulation threshold, whereas an 8–16 ha threshold was a better predictor in coarse-textured alluvial deposits. The optimal stream initiation threshold is thus variable depending on the type of landform and substrate and will further differ between applications:

Maximum NDVI, calculated over the growing seasons for ten years prior to disturbance, was also a significant predictor of vegetation regrowth following disturbance. Plots with higher pre-harvest NDVI showed greater post-harvest vegetation regrowth. Strong linkages exist between canopy light absorption, or greenness and environmental productivity, and researchers have integrated greenness over specific monthly periods, growing seasons, or for entire years to create surrogate variables for overall landscape productivity. These integrated indices of landscape greenness have been shown to be related to terrestrial net primary productivity (Goward et al., 1985), and are based on both a strong underlying theoretical basis and significant empirical correlations (Fung et al., 1987; Potter et al., 1993; Sellers, 1985) which hold across a variety of land cover types, including forests (Coops et al., 1998), grasslands (Wang, 2004), crops (Groten, 1993), as well as over a range of scales (Waring et al., 2006). Our results suggest

that pre-disturbance NDVI reflects some inherent aspects of site-level productivity allowing it to be a possible variable in pre-harvest site conditions. important for assessing post-harvest regeneration. This was particularly notable for the two deciduous-dominated forest types representing the earlier stages of succession, for which stands with higher pre-harvest NDVI showed much higher post-harvest regrowth. Additional work is required to further test these relationships along boreal mixedwood successional chronosequences, particularly in older stands, when much of the deciduous overstorey has been removed and the stand reaches a climax community.

We expected a relationship between productivity (as measured by pre-harvest NDVI) and depth to water that reflected the influence of moisture on productivity. Surprisingly, NDVI was positively related to depth to water, suggesting a negative relationship with site moisture. This is partly a reflection of variation in forest cover type because the two deciduous-dominated forest types, which were constrained to the drier end of the depth to water gradient, had higher NDVI values. Still, for the conifer and mixed forest types there was a notable decline in NDVI towards shallower depth to water. Thus, even though we constrained our study to merchantable 'upland' sites, avoiding lowland sites dominated by black spruce or tamarack, these results suggest some decline in productivity of these boreal forest types towards the wetter end of the soil moisture gradient. This could reflect the influence of a shallower aerobic rooting zone and/or cold soils that limit root growth, nitrogen mineralization and nutrient uptake (Lindo and Visser, 2003).

For both total canopy cover and vegetation regrowth, the best model included both site productivity (pre-treatment NDVI) and moisture (depth to water); the result confirms that the position of the plots within the edatopic grid is influential in terms of total canopy cover and regrowth following the harvesting treatments. Vegetation regrowth was greater for the two deciduous-dominated forest types and this likely reflects the rapid vegetative regeneration of aspen following disturbances. Interestingly, regrowth in these two forest types was greater towards the drier end of the depth to water gradient (higher depth to water). This was unexpected; however, trembling aspen, the dominant tree species in our deciduous-dominated forest types, is known to preferentially associate with drier sites (Albani et al., 2005; Bridge and Johnson, 2000). Our results suggest that within the moisture range of sites included in our study, forest regrowth following a disturbance such as variable retention harvesting may be poorer on moister sites. On the other hand, the influence of depth to water on vegetation regrowth in the mixed and conifer forests was relatively weak as compared to the deciduous-dominated forest types.

Variation in boreal mixedwood canopy composition from deciduous-dominated to mixed to conifer-dominated has often been viewed as a successional gradient reflecting time since disturbance (Chen and Popadiouk, 2002). However, there can be considerable variation in successional pathways for these forests with many possibilities for canopy composition at a given time since disturbance (Bergeron et al., 2014). The distribution of the four forest cover types across gradients of depth to water suggest that site conditions such as moisture and productivity could also have an influence on canopy composition of boreal mixedwood forests. This conforms with previous studies which have related plant distribution to soil moisture and nutrients and, in turn, topographic attributes such as hillslope position (Bridge and Johnson, 2000). Our observed pattern with the two deciduous-dominated forest types found on drier sites while mixed and conifer forests tended to be found on moister sites conforms to the results of Bridge and Johnson (2000) for distribution of boreal tree species across hillslope positions. Likewise, Albani et al. (2005) found that white spruce was associated with moister sites (channels, concave slopes) while hardwoods were positively associated with drier locations (ridges and convex slopes). Notable for our results was that the mixed and conifer forests covered a wide range of depth to water, including the drier end of the gradient to which deciduous-dominated forests were constrained.

5. Conclusion

Our results illustrate that recent advances in remote sensing technology can be useful for understanding landscape distribution of forest cover types and for predicting forest response to disturbance. Our results confirm that both Landsat-derived greenness (NDVI) and ALS – derived depth to water are related to forest cover type and can be used to predict the relative response of forest stands across gradients of productivity and moisture to variable retention harvesting.

Acknowledgements

This work was funded by a Natural Sciences and Engineering Research Council (NSERC) Strategic Grant to Ellen Macdonald and a NSERC Discovery grant to N. Coops. The ALS data were provided by Alberta Agriculture and Forestry as well as granting access to the wet areas mapping data. We are very grateful to all those involved in the establishment of the EMEND experiment, particularly John Spence and Jan Volney, and to all funders that made EMEND possible particularly: Daishowa-Marubeni International Ltd., Canadian Forest Products, Alberta Environment and Sustainable Resource Development, and Canadian Forest Service. V. Vartanian and Y. Lu are acknowledged for editorial assistance.

References

Ågren, A.M., Lidberg, W., Strömgren, M., Ogilvie, J., Arp, P.A., 2014. Evaluating digital terrain indices for soil wetness mapping – a Swedish case study. Hydrol. Earth Syst. Sci. 18, 3623–3634. http://dx.doi.org/10.5194/hess-18-3623-2014.

Akaike, H., 1973. Information theory and an extension of the maximum likelihood principle. In: Second Int. Symp. Inf. Theory, pp. 8–10.

Albani, M., Andison, D.W., Kimmins, J.P. (Hamish), 2005. Boreal mixedwood species composition in relationship to topography and white spruce seed dispersal constraint. For. Ecol. Manage. 209, 167–180. http://dx.doi.org/10.1016/j.foreco.2005.01.017.

Beckingham, J.D., Archibald, J.H., 1996. Field Guide to Ecosites of Northern Alberta.

Bergeron, Y., Chen, H.Y.H., Kenkel, N.C., Leduc, A.L., Macdonald, S.E., 2014. Boreal mixedwood stand dynamics: ecological processes underlying multiple pathways. For. Chron. 90, 202–213. http://dx.doi.org/10.5558/tfc2014-039.

Bergeron, Y., Gauthier, S., Kafka, V., Lefort, P., Lesieur, D., 2001. Natural fire frequency for the eastern Canadian boreal forest: consequences for sustainable forestry. Can. J. For. Res. 31, 384–391. http://dx.doi.org/10.1139/cjfr-31-3-384.

Bridge, S.R.J., Johnson, E.a., 2000. Geomorphic principles of terrain organization and vegetation gradients. J. Veg. Sci. 11, 57–70. http://dx.doi.org/10.2307/3236776.

Buddle, C.M., Langor, D.W., Pohl, G.R., Spence, J.R., 2006. Arthropod responses to harvesting and wildfire: implications for emulation of natural disturbance in forest management. Biol. Conserv. 128, 346–357. http://dx.doi.org/10.1016/j.biocon.2005.10.002.

Chen, H.Y., Popadiouk, R.V., 2002. Dynamics of North American boreal mixedwoods. Environ. Rev. 10, 137–166. http://dx.doi.org/10.1139/a02-007.

Clark, D.B., Palmer, M.W., 1999. Edaphic factors and the landscape-scale distributions of tropical rain forest trees. Ecology 80, 2662–2675.

Coops, N., Waring, R., Landsberg, J., 1998. Assessing forest productivity in Australia and New Zealand using a physiologically-based model driven with averaged monthly weather data and satellite-derived estimates of canopy photosynthetic capacity. For. Ecol. Manage. 104, 113–127.

Coops, N.C., Delahaye, A., Pook, E., 1997. Estimation of eucalypt forest leaf area index on the south coast of New South Wales using Landsat MSS data. Aust. J. Bot. 45, 757–769.

Coops, N.C., Hilker, T., Wulder, M.A., St-Onge, B., Newnham, G.J., Siggins, A., Trofymow, J.A., 2007. Estimating canopy structure of Douglas-fir forest stands from discrete-return LiDAR. Trees-Struct. Funct. 21, 295–310. http://dx.doi.org/10.1007/s00468-006-0119-6.

Coops, N.C., Wulder, M.A., Duro, D., Han, T., Berry, S.L., 2008. The development of a Canadian dynamic habitat index using multi-temporal satellite estimates of canopy light absorbance. Ecol. Indic. 8, 754–766. http://dx.doi.org/10.1016/j.ecolind.2008.01.007.

Fung, I.Y., Tucker, C.J., Prentice, K.C., 1987. Application of advanced very high resolution radiometer vegetation index to study atmosphere-biosphere exchange of CO_2. J. Geophys. Res. 92, 2999–3015.

Goward, S.N., Tucker, C.J., Dye, D.G., 1985. North American vegetation patterns observed with the NOAA-7 advanced very high resolution radiometer. Vegetatio 64, 3–14.
Groten, S.M.E., 1993. NDVI-crop monitoring and early yield assessment of Burkina Faso. Int. J. Remote Sens. 14, 1495–1515.
Haeussler, S., 2011. Rethinking biogeoclimatic ecosystem classification for a changing world. Environ. Rev. 19, 254–277.
Hannam, K., Quideau, S., Kishchuk, B., 2006. Forest floor microbial communities in relation to stand composition and timber harvesting in northern Alberta. Soil Biol. Biochem. 38, 2565–2575. http://dx.doi.org/10.1016/j.soilbio.2006.03.015.
Hannam, K.D., Quideau, S.A., Kishchuk, B.E., Oh, S.-W., Wasylishen, R.E., 2005. Forest-floor chemical properties are altered by clear-cutting in boreal mixedwood forest stands dominated by trembling aspen and white spruce. Can. J. For. Res. 35, 2457–2468. http://dx.doi.org/10.1139/X05-140.
Hansen, a.J., Spies, T.a., Swanson, F.J., Ohmann, J.L., 1991. Conserving biodiversity in managed forests. Bioscience 41, 382–392. http://dx.doi.org/10.2307/1311745.
Hermosilla, T., Wulder, M., White, J.C., Coops, N., Hobart, G.W., 2015. An integrated Landsat time series protocol for change detection and generation of annual gap-free surface reflectance composites. Remote Sens. Environ. 158, 220–234. http://dx.doi.org/10.1016/j.rse.2014.11.005.
Hilker, T., van Leeuwen, M., Coops, N.C., Wulder, M.A., Newnham, G.J., Jupp, D.L.B., Culvenor, D.S., 2010. Comparing canopy metrics derived from terrestrial and airborne laser scanning in a Douglas-fir dominated forest stand. Trees-Struct. Funct. 24, 1–14.
Hornberger, G.M., Boyer, E.W., 1995. Recent advances in watershed modelling. Rev. Geophys. 33, 949–957.
Huang, C., Goward, S.N., Masek, J.G., Thomas, N., Zhu, Z., Vogelmann, J.E., 2010. An automated approach for reconstructing recent forest disturbance history using dense Landsat time series stacks. Remote Sens. Environ. 114, 183–198. http://dx.doi.org/10.1016/j.rse.2009.08.017.
Hunter, M.L., 1993. Natural fire regimes as spatial models for managing boreal forests. Biol. Conserv. 65, 115–120.
Hylander, K., Dynesius, M., 2006. Causes of the large variation in bryophyte species richness and composition among boreal streamside forests. J. Veg. Sci. 17, 333–346.
Ise, T., Sato, H., 2008. Representing subgrid-scale edaphic heterogeneity in a large-scale ecosystem model: a case study in the circumpolar boreal regions. Geophys. Res. Lett. 35, L20407. http://dx.doi.org/10.1029/2008GL035701.
Jenson, S.K., Domingue, J.O., 1988. Extracting topographic structure from digital elevation data for geographic information system analysis. Photogramm. Eng. Remote Sens. 54, 1593–1600.
Jerabkova, L., Prescott, C.E., Kishchuk, B.E., 2006. Nitrogen availability in soil and forest floor of contrasting types of boreal mixedwood forests. Can. J. For. Res. 36, 112–122. http://dx.doi.org/10.1139/X05-220.
Kennedy, R.E., Yang, Z., Cohen, W.B., 2010. Detecting trends in forest disturbance and recovery using yearly Landsat time series : 1. LandTrendr—temporal segmentation algorithms. Remote Sens. Environ. 114, 2897–2910. http://dx.doi.org/10.1016/j.rse.2010.07.008.
Kishchuk, B.E., Quideau, S., Wang, Y., Prescott, C., 2014. Long-term soil response to variable-retention harvesting in the EMEND (Ecosystem Management Emulating Natural Disturbance) experiment, northwestern Alberta. Can. J. Soil Sci. 94, 263–279. http://dx.doi.org/10.4141/CJSS2013-034.
Kneeshaw, D., Gauthier, S., 2003. Old growth in the boreal forest: A dynamic perspective at the stand and landscape level. Environ. Rev. 11 (Suppl.), S99–S114. http://dx.doi.org/10.1139/A03-010.
Kraus, K., Pfeifer, N., 1998. Determination of terrain models in wooded areas with airborne laser scanner data. ISPRS J. Photogramm. Remote Sens. 53, 193–203.
Landsberg, J.J., 1996. Impact of climate change and atmospheric carbon dioxide concentration on the growth of planted forests. Greenhouse Coping Clim. Change, 205–219.
Lazaruk, L.W., Kernaghan, G., Macdonald, S.E., Khasa, D., 2005. Effects of partial cutting on the ectomycorrhizae of *Picea glauca* forests in northwestern Alberta. Can. J. For. Res. 35, 1442–1454. http://dx.doi.org/10.1139/X05-062.
Lefsky, M.A., Cohen, W.B.W., Acker, S.A., Parker, G.G.G., Spies, T.A., Harding, D., 1999. Lidar remote sensing of the canopy structure and biophysical properties of Douglas-fir western hemlock forests. Remote Sens. Environ. 70, 339–361.
Levin, S.A., 2012. Multiple scales and the maintenance of biodiversity. Ecosystems 3, 498–506. http://dx.doi.org/10.1007/s100210000044.
Lindo, Z., Visser, S., 2003. Microbial biomass, nitrogen and phosphorus mineralization, and mesofauna in boreal conifer and deciduous forest floors following partial and clear-cut harvesting. Can. J. For. Res. 33, 1610–1620. http://dx.doi.org/10.1139/X03-080.
Loveland, T.R., Dwyer, J.L., 2012. Landsat: building a strong future. Remote Sens. Environ. 122, 22–29. http://dx.doi.org/10.1016/j.rse.2011.09.022.
Macdonald, S.E., Fenniak, T.E., 2007. Understory plant communities of boreal mixedwood forests in western Canada: natural patterns and response to variable-retention harvesting. For. Ecol. Manage. 242, 34–48. http://dx.doi.org/10.1016/j.foreco.2007.01.029.
Major, J., 1951. A functional, factorial approach to plant ecology. Ecology 32, 392–412.
Masek, J.G., Huang, C.Q., Wolfe, R., Cohen, W.B., Hall, F., Kutler, J., 2008. North American forest disturbance mapped from a decadal Landsat record. Remote Sens. Environ. 112, 2914–2926.
Masek, J.G., Vermote, E.F., Saleous, N.E., Wolfe, R., Hall, F.G., Huemmrich, K.F., Gao, F., Kutler, J., Lim, T.K., 2006. A Landsat surface reflectance dataset for North America, 1990–2000. Geosci. Remote Sens. Lett. IEEE 3, 68–72.
Murphy, P.N.C., Ogilvie, J., Arp, P., 2009. Topographic modelling of soil moisture conditions: a comparison and verification of two models. Eur. J. Soil Sci. 60, 94–109. http://dx.doi.org/10.1111/j.1365-2389.2008.01094.x.
Murphy, P.N.C., Ogilvie, J., Castonguay, M., Zhang, C.F., Meng, F.R., Arp, P.a., 2008a. Improving forest operations planning through high-resolution flow-channel and wet-areas mapping. For. Chron. 84, 568–574.
Murphy, P.N.C., Ogilvie, J., Meng, F., Arp, P., 2008b. Stream network modelling using lidar and photogrammetric digital elevation models: a comparison and field verification. Hydrol. Process. 22, 1747–1754. http://dx.doi.org/10.1002/hyp.
Næsset, E., 2004. Effects of different flying altitudes on biophysical stand properties estimated from canopy height and density measured with a small-footprint airborne scanning laser. Remote Sens. Environ. 91, 243–255.
Naesset, E., 1997. Estimating timber volume of forest stands using airborne laser scanner data. Remote Sens. Environ. 61, 246–253.
Næsset, E., Gobakken, T., 2008. Estimation of above-and below-ground biomass across regions of the boreal forest zone using airborne laser. Remote Sens. Environ. 112, 3079–3090.
Nijland, W., Coops, N.C., Macdonald, S.E., Nielsen, S.E., Bater, C.W., Stadt, J., 2015. Comparing patterns in forest stand structure following variable harvests using airborne laser scanning data. For. Ecol. Manage. http://dx.doi.org/10.1016/j.foreco.2015.06.005.
Pogrebnjak, P.S., 1929. {Ü}ber die Methodik der Standortsuntersuchungen in Verbindung mit den Waldtypen.
Pojar, J., Klinka, K., Meidinger, D., 1987. Biogeoclimatic ecosystem classification in British Columbia. For. Ecol. Manage. 22, 119–154.
Potter, C.S., Randerson, J.T., Field, C.B., Matson, P.A., Vitousek, P.M., Mooney, H.A., Klooster, S.A., 1993. Terrestrial ecosystem production: a process model based on global satellite and surface data. Global Biogeochem. Cycles 7, 811–841.
Rysin, L.P., 1982. Forest Typology in USSR.
Saunders, D.A., Hobbs, R.J., Margules, C.R., 1991. Biological consequences of ecosystem fragmentation: a review. Conserv. Biol. 5, 18–32.
Seibert, J., Stendahl, J., Sørensen, R., 2007. Topographical influences on soil properties in boreal forests. Geoderma 141, 139–148. http://dx.doi.org/10.1016/j.geoderma.2007.05.013.
Sellers, P.J., 1985. Canopy reflectance, photosynthesis and transpiration. Int. J. Remote Sens. 6, 1335–1372. http://dx.doi.org/10.1080/01431168508948283.
Tucker, C.J., 1979. Red and photographic infrared linear combinations for monitoring vegetation. Remote Sens. Environ. 8, 127–150.
Turner, M.G., 1989. Landscape ecology: the effect of pattern on process. Annu. Rev. Ecol. Syst. 20, 171–197.
Vermote, E.F., El Saleous, N., Justice, C.O., Kaufman, Y.J., Privette, J.L., Remer, L., Roger, J.C., Tanré, D., 1997. Atmospheric correction of visible to middle-infrared EOS-MODIS data over land surfaces: background, operational algorithm and validation. J. Geophys. Res. 102, 17131–17141. http://dx.doi.org/10.1029/97JD00201.
Volney, W.J.A., Hammond, H.E.J., Maynard, D.G., MacIsaac, D.A., Mallett, K.I., Langor, D.W., Johnson, J.D., Pohl, G.R., Kishchuk, B., Gladders, B., Avery, B., Chemago, R., Hoffman, T., Chorney, M., Luchkow, S., Maximchuck, M., Spence, J.R., 1999. A silvicultural experiment to mitigate pest damage. For. Chron. 75, 461–465.
Wang, S., 2004. One hundred faces of sustainable forest management. For. Policy Econ. 6, 205–213. http://dx.doi.org/10.1016/j.forpol.2004.03.004.
Waring, R.H., Coops, N.C., Fan, W., Nightingale, J.M., 2006. MODIS enhanced vegetation index predicts tree species richness across forested ecoregions in the contiguous USA. Remote Sens. Environ. 103, 218–226.
White, B., Ogilvie, J., Campbell, D.M.H.M.H., Hiltz, D., Gauthier, B., Chisholm, H.K.H., Wen, H.K., Murphy, P.N.C.N.C., Arp, P.A.A., 2012. Using the cartographic depth-to-water index to locate small streams and associated wet areas across landscapes. Can. Water Resour. J. 37, 333–347. http://dx.doi.org/10.4296/cwrj2011-909.
White, J.C., Wulder, M.A., Vastaranta, M., Coops, N.C., Pitt, D., Woods, M., 2013. The utility of image-based point clouds for forest inventory: a comparison with airborne laser scanning. Forests 4, 518–536. http://dx.doi.org/10.3390/f4030518.
Work, T.T., Shorthouse, D.P., Spence, J.R., Volney, W.J.a., Langor, D., 2004. Stand composition and structure of the boreal mixedwood and epigaeic arthropods of the Ecosystem Management Emulating Natural Disturbance (EMEND) landbase in northwestern Alberta. Can. J. For. Res. 34, 417–430. http://dx.doi.org/10.1139/x03-238.
Wulder, M.a., Masek, J.G., Cohen, W.B., Loveland, T.R., Woodcock, C.E., 2012. Opening the archive: how free data has enabled the science and monitoring promise of Landsat. Remote Sens. Environ. 122, 2–10. http://dx.doi.org/10.1016/j.rse.2012.01.010.
Wulder, M.A., Bater, C.C.W., Coops, N.C., Hilker, T., White, J.C., 2008a. The role of LiDAR in sustainable forest management. For. Chron. 84, 807–826.
Wulder, M.A., White, J.C., Cranny, M.M., Hall, R.J., Luther, J.E., Beaudoin, A., Goodenough, D.G., Dechka, J.A., 2008b. Monitoring Canada' s forests. Part 1: Completion of the EOSD land cover project. Can. J. Remote Sens. 34, 549–562.
Zhu, Z., Woodcock, C.E., 2012. Object-based cloud and cloud shadow detection in Landsat imagery. Remote Sens. Environ. 118, 83–94. http://dx.doi.org/10.1016/j.rse.2011.10.028.
Zhu, Z., Woodcock, C.E., Olofsson, P., 2012. Continuous monitoring of forest disturbance using all available Landsat imagery. Remote Sens. Environ. 122, 75–91. http://dx.doi.org/10.1016/j.rse.2011.10.030.